Physica B 406 (2011) 3752–3758

Contents lists available at ScienceDirect

Physica B

journal homepage: www.elsevier.com/locate/physb

The effect of crystal lattice distortions on the electronic band structure and optical properties of the N,V- and N,Na-doped anatase

V.P. Zhukov *, V.M. Zainullina

Institute of Solid State Chemistry, Urals Branch of the Russian Academy of Sciences, 620990 Yekaterinburg, Russia

ARTICLE INFO

Article history:
Received 31 May 2011
Received in revised form
23 June 2011
Accepted 24 June 2011
Available online 8 July 2011

Keywords:
Dilute magnetic semi-conductors
LMTO
Quantum Espresso
LSDA+U
Electronic band structure
Anatase
Doping
Photocatalyses

ABSTRACT

The crystal structure, energy band structure and optical absorption of the N,V-doped and N,Na-doped anatase are studied by means of the first-principle pseudo-potential plane wave and linear muffin-tin orbitals methods. We show that the nitrogen and vanadium atoms have a tendency to form covalently bonded pairs. The crystal lattice distortions associated with doping essentially affect the optical absorption. With doping the impurity bands emerge in the band gap of the host anatase, however, a noticeable increase of optical absorption takes place at the energy only above 3 eV. Possible impact of this effect on the photocatalytic activity of the doped anatase is outlined.

1. Introduction

It has been found more than three decades ago that the titanium dioxide in the anatase structure, a semi-conductor with the band gap of 3.2 eV, is a good photocatalyst in the ultra-violet region of the sunlight [1,2]. Since then many efforts have been devoted to extending its photocatalytic activity to the visible part of the spectrum [3]. The photocatalytic activity essentially depends on the efficiency of the light absorption, hence, it is affected by the spectra of electronic states nearby the band gap. When a semi-conductor absorbs a photon with the energy above the band gap, an electron–hole pair is generated, with photocatalytically active electron inside the conduction band and hole inside the valence band. In order to obtain a photocatalyst effective in the visible range, one has to create such crystal structure that has an absorption in the energy interval from 1.6 to 3.0 eV. One of the successful methods for this purpose is the doping with s-, p- or d-elements, see, e.g. reviews [4–7]. The doping can introduce impurity states inside the band gap of the pure anatase, thus reducing the band gap and favoring the improvement of the photocatalytic properties. Based on this idea, a series of experimental works has been carried out with doping by boron [8], carbon [9,10], nitrogen [11], aluminum [12], vanadium [13,10], chromium and iron [13]. In many cases an increase of absorption in optical region has been revealed correlated with the rise of the photocatalytic activity, however, the search for the better kinds of doping is still in progress.

Since the photocatalytic activity depends on the electronic band structure, a very appealing idea is to employ the first-principle methods for evaluating the band structure and optical absorption. For anatase doped with boron such researches have been performed in the works [8,14–16]. Analogous calculations have been done for anatase doped with carbon [11,17–20]. The most extensive calculations have been performed for doping with nitrogen [11,18,21–26]. However, because of some essential shortcomings the effectiveness of the first-principle researches is far from being sufficient. In the most part of the works the results were obtained by means of the methods of the density-functional theory. A well known drawback of such approaches is an essential underestimation of the band gap that makes problematic comparison with experimental optical data. Only in the works [19,20] the calculated value of the band gap was corrected by means of the LDA+U approach. Neglecting the crystal lattice relaxation around impurity atom was also a frequently used simplification. Furthermore, the most essential shortcoming is probably that the estimation of the optical absorption in the doped compounds was performed on a qualitative level only, by examining the energy and composition of the impurity bands

* Corresponding author. Tel.: +7 343 362 33 77; fax: +7 343 374 44 95.
E-mail address: zhukov@ihim.uran.ru (V.P. Zhukov).

0921-4526/$ - see front matter © 2011 Elsevier B.V. All rights reserved.
doi:10.1016/j.physb.2011.06.089

inside the band gap. The validity of such an approach neglecting transition probabilities is a questionable issue. The first-principle calculations of the optical absorption in the doped semi-conductors, although feasible, encounter numeric problems, so only in the papers of Asahi et al. [11], Zhao et al., [26] the results of calculations for the dielectric function of N-doped anatase were presented, whereas Zainullina et al. [19,20] discussed dielectric function of the V,C-doped anatase. However, since in the works of Asahi et al. and Zhao et al. the calculated band gap was too narrow, and in the works of Zainullina et al. the crystal lattice relaxation around the impurity atom was neglected, these papers are not sufficient for a judgement about the validity of the mentioned qualitative approach.

In view of these circumstances, we have performed a new research on the electronic band structure and optical absorption in some doped anatase compounds. The choice of the objects under study was based on the following considerations. One of the mostly studied photocatalysts manifesting activity in visible part of spectra is the nitrogen-doped anatase [11]. Its band structure has, however, a number of disadvantages that restrict the photocatalytic activity. As first-principle calculations demonstrate the partly occupied bands of nitrogen atoms are hybridized with the oxygen states and have the energy very close to the top of the valence band [11]. So the gap between the occupied N states and conduction band is only slightly less than in the pure anatase. The visible light absorption in the N-doped anatase is provided mainly by the excitations from the valence band states to empty nitrogen states, with much smaller contribution of the excitations to the conduction band [27]. Therefore the photocatalytic activity of the N-doped anatase under visible light is determined mainly by the heavy electrons in nitrogen band states and heavy holes in the valence band, whereas for a high photocatalytic activity one should have the carriers with high mobility.

An evident idea of improving the photocatalytic activity is the filling of the empty nitrogen states with additional electrons. A first positive consequence would be the change of the type of carriers, from heavy electrons in the nitrogen band to light electrons in the conduction band. A second consequence would be the rise of the energy of nitrogen states accompanied by the reduction of the band gap. One more expected consequence would be the reduction of the recombination time of the excited electron–hole pairs because of the elimination of the electron drops from the conduction band states to the nitrogen states.

One can imagine two hypothetical ways of filling the nitrogen states. First way is to perform the replacement of the titanium atoms with the donor atoms of formal valency $+5$, e.g. vanadium. A similar double doping of anatase, with carbon and vanadium, has been earlier performed by the authors of the papers [9,10]. A second way is to perform the implantation of the donor atoms with formal valency $+1$, e.g. sodium, in the interstitial sites of the anatase crystal. We are not aware about the experiments on sodium intercalation in anatase, but the intercalation of the $+1$ hydrogen and lithium is a well developed branch of researches [24,28–31].

So we have performed a first-principle theoretical research of the electronic structure and optical properties of the anatase doped with nitrogen and vanadium, nitrogen and sodium. The calculations included optimization of the crystal structure of the doped compounds and the corrections (LDA+U) necessary to treat the problem of too narrow band gap. The dielectric function and coefficient of optical absorptions have been calculated. In the following sections we discuss the details of the calculations, the effect of crystal lattice distortion on the band structure and optical properties and the implications for the photocatalytic activity.

2. Theory

The intensity of light absorption in a solid is determined by its dielectric function [32]. We use for the calculations of dielectric function an *ab initio* approach that follows from the many-body theory of solids [33–35]. The calculations are based on the proved in this theory exact relation between the *inverse* dielectric function ε^{-1}, bare Coulomb potential V and response function R:

$$\varepsilon^{-1}(1,2)=\delta(1-2)+\int d(3)V(1,3)R(3,2) \tag{1}$$

We employ afterwards the abbreviations similar to $1\equiv \mathbf{r_1},t_1$. Also a polarization function P is defined in many-body theory in such a way that the dielectric function satisfies to the equation

$$\varepsilon(1,2)=\delta(1-2)-\int d(3)V(1,3)P(3,2) \tag{2}$$

These definitions permit to connect the response and polarization functions via a Dyson-like equation

$$R(1,2)=\int d(3)P(1,3)\varepsilon^{-1}(3,2)=P(1,2)+\int d(3)d(4)P(1,3)V(3,4)R(4,2) \tag{3}$$

The calculations of polarization function present a very difficult problem of the many-body theory whose exact solution is still not feasible. Fortunately, a rather correct approach is in many cases the "random phase" approximation (RPA) which is exact in the limit of infinitely small electron density parameter r_s [33–35]. Based on the RPA one comes to the two ways of calculating the dielectric function. First way is to employ directly Eq. (2). It has been shown [36] that this way of calculations does not take into account the so-called local fields, that is the fourier components of the internal field in solid with wave vectors different from the wave vector of the external applied potential. Although it is preferable for homogenies systems, only this approach was used before in the calculations for the dielectric function of the pure and doped anatase. The second way is to solve Eq. (3) with respect to the response function, then to substitute R into Eq. (1), to find ε^{-1} and invert it. As it has been shown in Ref. [36], this way, although longer, incorporates local field effects, so it is preferable for strongly inhomogeneous systems. Since anatase is just a such case, we prefer to employ this second approach, although near the end of the paper we submit some data concerning the effect of local fields on the dielectric function.

The calculations for real solids are usually performed by expanding the polarization and related quantities into a series of a complete basis set of Bloch functions. Since in the case of the doped anatase the calculations are carried out for big super-cells, highly desirable is to employ a basis set as short as possible. A very efficient proves to be the set of the so-called basic product-states composed of the linear muffin-tin orbitals which was proposed by Aryasetiawan and Gunnarsson [37]. Normally this set is very short, some tens of the states per atom, nevertheless it provides sufficiently correct results both for non-magnetic and magnetic systems [38,39]. If we denote such basic functions as $|B_{\mathbf{q},i}\rangle$, then the fourier transform of the polarization matrix in the RPA approximation is written in the Bloch-function basis as [37]

$$\mathbf{P}^0_{i,j}(\mathbf{q},\omega)=\sum_{\sigma,t,\mathbf{k}}\sum_{n}^{occ}\sum_{n'}^{unocc}\frac{1}{t\omega-\varepsilon_{\mathbf{k}+\mathbf{q},n',\sigma}+\varepsilon_{\mathbf{k},n,\sigma}+i\delta}\times\langle B_{\mathbf{q},i}\psi_{\mathbf{k},n,\sigma}\mid\psi_{\mathbf{k}+\mathbf{q},n',\sigma}\rangle\langle\psi_{\mathbf{k}+\mathbf{q},n',\sigma}\mid\psi_{\mathbf{k},n,\sigma}B_{\mathbf{q},j}\rangle \tag{4}$$

The summation includes terms with $t=\pm 1$ (electrons and holes) and spin value σ; $\psi_{\mathbf{k},n}$ are one-particle wavefunction of the occupied states and $\psi_{\mathbf{k}+\mathbf{q},n'}$ are wavefunctions of the empty states. Hence, polarization function contains contributions of all possible electron excitations, and its imaginary part is proportional to the

number of excited electron–hole pairs. In such representation the local fields incorporating calculations of the dielectric function for any given wave vector $\mathbf{q}$ and frequency ω are converged to the solution of the equation for the matrix of the response function

$$R(\mathbf{q},\omega) = P^0(\mathbf{q},\omega) + P^0(\mathbf{q},\omega)V(\mathbf{q})R(\mathbf{q},\omega) \quad (5)$$

With the calculated P^0 and R matrices the calculations of the macroscopic ε and ε^{-1} values according to the Eqs. (1) and (2) are reduced to

$$\varepsilon(\mathbf{q},\omega) = 1 - \frac{4\pi}{\mathbf{q}^2}\sum_{i,j} \langle \mathbf{q}|B_{\mathbf{q}i}\rangle P^0_{i,j} \langle B_{\mathbf{q}j}|\mathbf{q}\rangle \quad (6)$$

and

$$\varepsilon^{-1}(\mathbf{q},\omega) = 1 + \frac{4\pi}{\mathbf{q}^2}\sum_{i,j} \langle \mathbf{q} \mid B_{\mathbf{q}i}\rangle R_{i,j} \langle B_{\mathbf{q}j} \mid \mathbf{q}\rangle \quad (7)$$

where the factors $4\pi/\mathbf{q}^2$ are the fourier transforms of the bare Coulomb potential. First the imaginary part of polarization is calculated via Eq. (4) and then the real part of polarization via the Kramers–Kronig transform. Then the matrix equation (5) is solved for R with $\mathbf{q}$ and ω in the range of interest. Finally real (ε_1) and imaginary (ε_2) parts of dielectric function are calculated. In more details such calculations are discussed in the review [37]. Having $\varepsilon = \varepsilon_1 + i\varepsilon_2$ it is easy task to calculate the reflection and absorption coefficients [32]. In our study we calculated the absorption coefficient

$$K(\mathbf{q},\omega) = 2\omega k(\mathbf{q},\omega)/c \quad (8)$$

where k is the imaginary part of the complex wave vector $N = \sqrt{\varepsilon}$ of light in solid.

3. Details of calculations

The anatase structure of titanium dioxide has tetragonal body-centered lattice (space group $I4_1/amd$, $Z=4$), and the values of crystal lattice parameters are $a=b=3.7845$ Å, $c=9.5143$ Å, $u=0.20806$ [40]. The tetragonal unit cell of anatase contains four titanium atoms in the 4a positions and eight oxygen atoms in the 8e positions. The nearest coordination sphere of a titanium atom is a distorted octahedron of eight oxygen atoms, whereas the nearest coordination sphere of an oxygen atom is a distorted triangle of titanium atoms, see Fig. 1.

The $(2\times2\times2)$ $Ti_{16}O_{32}$ super-cell was used in the calculations obtained by means of the twofold translations of the primitive unit cell Ti_2O_4 along all the three vectors of primitive translations. The simulation of the N-doping was performed via the replacement of an oxygen atom with nitrogen atom. The V-doping was modeled by the replacement of one titanium atom with vanadium atom. This replacement corresponds to the compound $Ti_{1-x}V_xO_{2-x}N_x$ with $x = 1/16$, hence to 6.250% of oxygen sublattice substitution. Three different arrangements of the vanadium atom with respect to the nitrogen atom have been studied—see discussion in the next section. A preliminary choice of the interstitial site for the sodium atoms was performed by means of the tools provided by the tight-binding linear muffin-tin orbital (TB-LMTO) computer code [41]. This code permits to estimate the radii of atomic spheres by searching for the minima of the overlapping Hartree atomic potentials. The empty-sphere pseudo-atoms with basic LMTO's are introduced into the regions not covered by the atomic spheres, and finally all the radii are scaled in order to fill the whole space of crystal. We assumed that the sodium atom can occupy the empty-sphere site that has the biggest radius and the lowest number of the neighbor atoms. Such sphere, whose radius is bigger than the radius of the Ti sphere, is located in the center of Ti_4 square in the ab-plane, see Fig. 1. In more details the location of the Na atom is discussed in the next section.

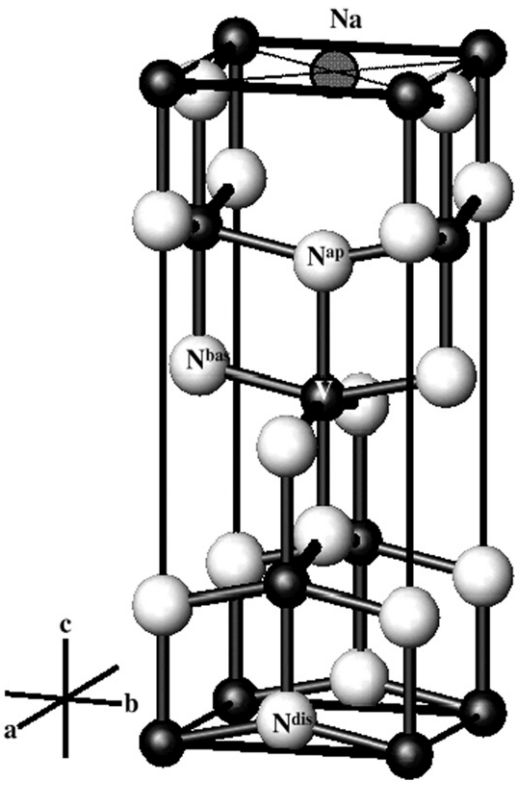

Fig. 1. A fragment of the anatase structure of titanium dioxide. The titanium and vanadium atoms are shown in black, oxygen and nitrogen atoms are in light gray, and the position of the doping sodium atom is in dark gray. The locations of the nitrogen atoms replacing oxygen atoms and vanadium atoms replacing titanium atoms are also marked.

The calculations of the electronic band structure and optical characteristics were performed using the TB-LMTO method [42] with the account of the on-site Coulomb correlations (LDA+U) [43]. In comparison with the pseudo-potential plane-wave methods mainly used before in the *ab initio* studies of the doped anatase, such an approach has a number of advantages. First of them is the minimal length of the employed basis set, no more than nine LMTO's per Ti, V, N or O atom. The second advantage is the possibility to construct from the products of LMTO's a very short set of basis function $B_{\mathbf{q}j}$ for the calculations of P, R, ε, ε^{-1}, typically no more than 40 product-functions per one atom [36]. This makes possible the calculations of the electronic band structure and dielectric function taking into account the local fields for crystals with very big unit cells. With a proper choice of the parameters U,J of the on-site Coulomb interactions [19,20] it appears to be possible to obtain the correct value of the band gap, and also to calculate the energy of the impurity bands in anatase in a good agreement with experiment.

A drawback of the TB-LMTO approach is an insufficiently high precision of the calculations for the total ground state energy, hence such an approach cannot be used for evaluation of crystal lattice relaxation in the neighborhood of the doping atoms. Therefore before the LMTO calculations we evaluated the relaxed crystal structure using the density-functional perturbation theory [44] implemented in the pseudo-potential Quantum Espresso (QE) computer code [45]. In the calculations of electronic states the pseudo-potentials provided by the QE computer code were employed. For Ti and V atoms they were the Vanderbilt ultrasoft pseudo-potentials calculated with Perdew–Burke–Ernzerhof (PBE) exchange-correlation potential. For N and O atoms we used

the Rabe-Rappe-Kaxiras-Joannopoulos ultrasoft pseudo-potentials evaluated with the PBE exchange-correlation potential. For sodium they were of the same type as for titanium. The $4\times4\times4$ Monkhorst-Pack grid of 18 wave vectors and a plane-wave basis set with the energy cutoff of 40 Ry were employed in the calculations. Total optimization of the crystal structure parameters of the pure anatase has resulted in very small deviations from the experimental data, generally less than 0.5%. For instance, the calculated a-period of the lattice was 3.7832 Å, only 0.03% deviation from the experimental value. So we believe that our choice of the parameters of calculations is adequate for obtaining reliable data on the geometry of the crystals. In the calculations of the geometry of the doped compounds we kept the lattice units of the super-cell fixed and relaxed atomic coordinates only.

The optimized atomic coordinates were employed in the following TB-LMTO calculations. The grid of 64 wave vectors per full Brillouine zone of the super-cell was employed in these calculations. The basis set included the 4s-, 4p-, 3d-orbitals of Ti and 2s-, 2p-orbitals of oxygen and nitrogen atoms, 3s-states of the Na atoms. Since the structure of TiO_2 is rather friable, a set of 80 additional empty-sphere pseudo-atoms (E) occupying positions with minimum charge density has been added to the $(2\times2\times2)$-super-cell; only s-states of the E-pseudo-atoms were included in the basis set. The 3d-states of N, O atoms, 3p- and 3d-states of Na atoms, p- and d-states of the E-pseudo-atoms were referred to the so-called intermediate states whose effect on the electronic structure has been included via the "down-folding" perturbation theory [42]. In the LDA+U calculations the values of the Coulomb correlation parameter $U=6.2$ eV and of exchange parameter $J=0.7$ eV have been taken for Ti atoms from our previous calculations [19,20], whereas for V atoms they were 3.6 and 0.88 eV, respectively.

Based on the electronic band structure calculated via TB-LMTO method the calculations of the RPA polarization function, response function, inverse and direct dielectric functions have been carried out in the basis of LMTO product-orbitals [36,46]. The calculations were performed for the wave vector of minimum length of our grid of the LMTO wave vectors. This was the vector displaced from the Γ point by 1/8 of the $\Gamma-N$ direction. The product-orbitals have been constructed from the products of 2p-LMTO's of O and N atoms, 3d-LMTO's of Ti and V atoms and 3s-LMTO's of Na atoms, hence the products of the $2p\times2p$ and $2p\times3d$ kinds [47] were used. This makes possible to take into account the excitations between the valence band states, impurity band states of the doping atoms and conduction band states. In these calculations the contributions of intermediate states were neglected. Finally, the absorbtion coefficient was calculated according to Eq. (8).

4. Results and discussion

In our previous papers [10,19,20] the effects of replacement of oxygen and titanium atoms of anatase with carbon and vanadium atoms have been studied. It has been shown that the carbon and vanadium atoms display a trend of forming a covalently bonded dipoles with the shortest distance between these atoms. We assumed that in the case of the vanadium and nitrogen doping a similar effect can take place, so we performed the band-structure calculations for three various arrangements of the doping nitrogen atom with respect to the doping vanadium atom, see Fig. 1. The first arrangement is such that the nitrogen atom (N^{bas}) replaces the oxygen atom in the basal (ab) plane higher than the plane of V atoms by $0.051a$. The second is such that the nitrogen atom (N^{ap}) is in apical position with respect to the vanadium atom. In these cases the distance between the V and N non-relaxed positions is 1.934 and 1.979 Å, respectively. With the third arrangement the nitrogen atom (N^{dis}) is as far from the vanadium atom as it is possible with the $(2\times2\times2)$ super-cell; the V–N distance is in this case equal to 5.492 Å. The optimized energy of the super-cell, as it follows from the QE calculations, is equal for the three arrangements to -2908.41769 Ry (arr. 1), -2908.40782 Ry (arr. 2) and -2908.36497 Ry (arr. 3). Hence, the calculations show that the arrangements 1 and 2, with the shortest V–N distances, are energetically more favorable than the arrangement 3 with separated atoms. We will show below that this is a consequence of the covalent V–N bonding. The energy of dissociation of the V–N dipole evaluated as the difference of the total energies $E_d=E_{tot}(\text{arr.3})-E_{tot}(\text{arr.1}\vee\text{arr.2})$ is, respectively, 0.718 and 0.584 eV, comparable with the energy of the V–C bonding in anatase, 1.33 eV [19]. Because of the much higher total energy of the third arrangement we believe that this arrangement is less realizable, so we discuss hereafter the results for the first and second arrangements only.

In order to demonstrate the crystal lattice relaxation with doping we show in Fig. 2 geometric parameters for the fragments of the structure of the pure anatase, V,N-doped and Na,N-doped anatase. The main difference between the geometry of the pure and V,N-doped anatase is the much shorter V–N bond length in comparison with the Ti–O bond length, the effect correlating with the strong V–N bonding. As for the sodium atom, this atom also suffers a shift from the preliminary chosen position in the center of the Ti_4 squares, the choice discussed in the previous section. The preliminary chosen position coincides with the center of an O_4-tetrahedron greatly flattened in the c-direction. In the course of the QE crystal lattice optimization the sodium atom moves down and finally occupies position between the two lower oxygen atoms of the tetrahedron, such that the fragment O–Na–O becomes almost linear. The optimized geometry for the nearest surrounding of the sodium atom is also shown in Fig. 2. The downward shift of the sodium atom can be refereed to the strengthening of ionic bonding between sodium and oxygen atoms. On the other hand,

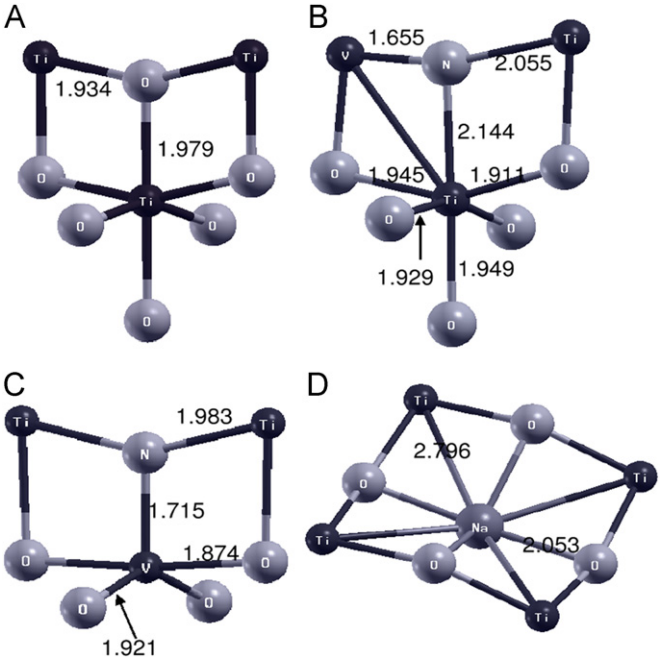

Fig. 2. The nearest surroundings of the doping atoms in the anatase crystal. (A) Pure anatase; (B) V,N-doped anatase with the first (basal) V and N atoms arrangement; (C) V,N-doped anatase with the second (apical) V and N-arrangement; (D) the nearest surrounding of sodium atom in Na,N-doped anatase. The interatomic distances are shown in Å units.

the Na–O distances, 2.053 Å, are longer than all the shortest TiO distances in pure anatase, the effect that can be interpreted as a result of the O–Na repulsion because of the big radius of the Na atom.

The changes of the geometry of crystals, although seemingly small, noticeably change the electronic band structure. In order to demonstrate this, we show in Fig. 3 the densities of states (DOS) for the pure and N,V-doped anatase, both for the crystal lattice relaxation neglected and taken into account. The main effect of doping consists in the occurrence of impurity bands inside the band gap of the pure anatase, near the top of the valence band and near the bottom of the conduction band. The DOS of the impurity states near the top of the valence band has a tail inside the valence band, so these states are hybridized with the oxygen 2p states, whereas the DOS of the states near the bottom of the conduction band has a tail inside the conduction band, so these states are hybridized with the Ti 3d-states. The percentage of the contributions to the lower impurity bands is about 15%V: 40%N:44%O for first arrangement and 16%V:21%N:62%O for the second arrangement. The effect of relaxation on the band structure consists in a noticeable decrease of the energy of the lower impurity bands and an increase of the energy of the higher impurity bands. Hence, taking into account the mixing of the V and N states, one may conclude that the lower impurity bands are bonding with respect to V–N interactions, whereas the higher impurity bands are their antibonding counterparts. When the relaxation is included, the gap between the top of the lower impurity band and the bottom of the higher impurity band is for

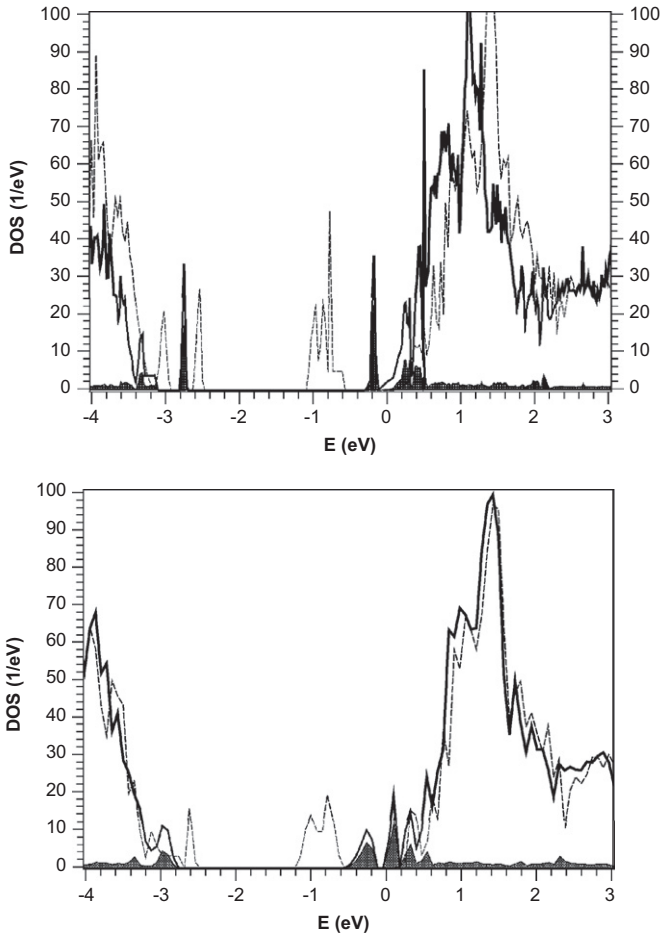

Fig. 3. Total and partial densities of states for the V,N-doped anatase. With dashed lines the total densities of states are shown for the crystal lattice relaxation neglected, whereas with solid lines the similar data for the relaxation taken into account are shown. The area filled with black corresponds to the partial density of states of V and N atoms. Upper and lower panel are, respectively, for the first and second arrangements of the vanadium and nitrogen atom.

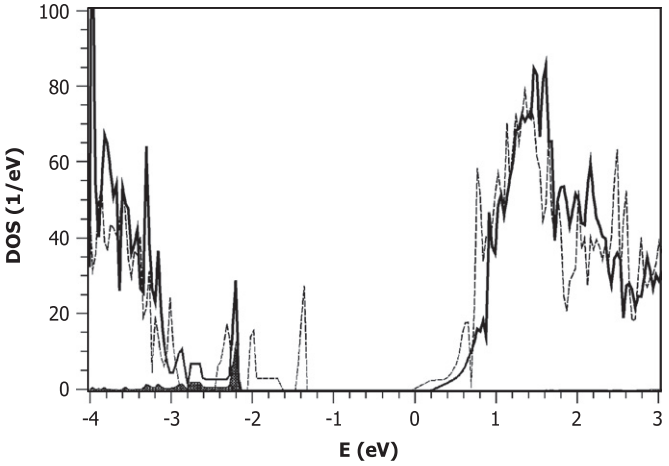

Fig. 4. Densities of states in Na,N-doped anatase. Notations are as in Fig. 3.

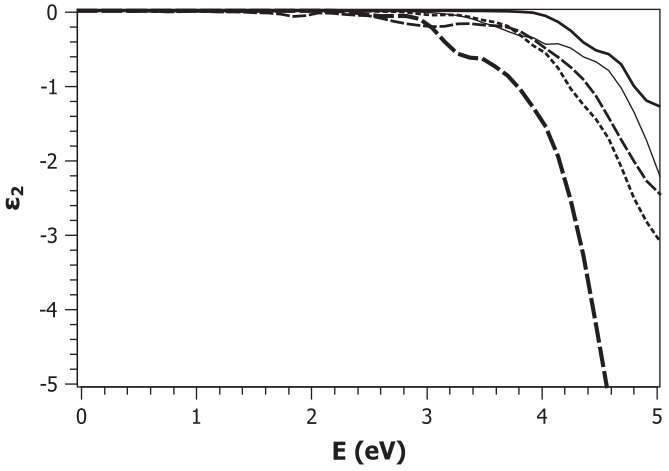

Fig. 5. Imaginary part of dielectric function for pure anatase, V,N-doped and N,Na-doped anatase. With thick solid line the data for pure anatase are shown. With thin solid line the data for the first arrangement of the V and N atoms are given. Thick dashed line represents the data for the second arrangement of the V and N atoms with lattice relaxation taken into account, whereas thin dashed line is for the lattice relaxation neglected. The dot line represents the data for N,Na-doping.

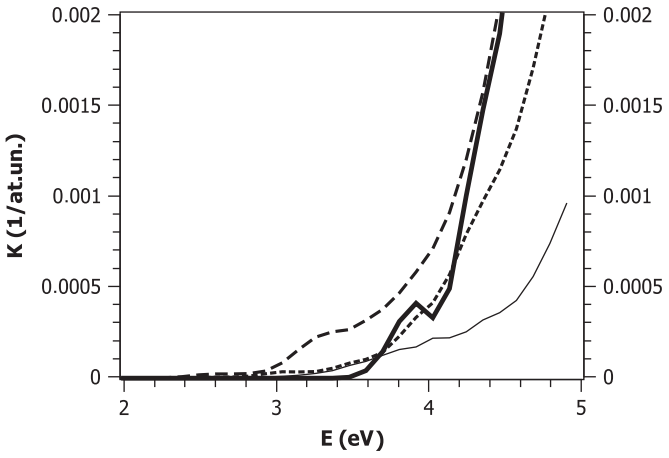

Fig. 6. Absorption coefficient for pure anatase, V,N-doped and N,Na-doped anatase. Destination of the lines is as in Fig. 5.

the first V,N arrangement equal to 2.4 eV, and for second arrangement it is 2.2 eV. Hence, one may anticipate in this case a light absorption favoring the photocatalytic activity in visible range, but we will see afterwards that such absorption in fact is weak.

In Fig. 4 we show the DOS's for the Na,N-doped anatase, with relaxation effects both disregarded and taken into account. Comparing with the case of only N-doping [11,18,21–26], one can see that the addition of one more electron to the lower impurity band gives rise to a great shift of this band to higher energy. Unfortunately, the effect of relaxation noticeably reduces this effect, but finally the Fermi level is still 0.6 eV above the top of the valence band. This corresponds to the gap between the Fermi level and the bottom of the conduction band equal to 2.4 eV, so the absorption in visible range can be also expected, but we will see that in fact this absorption also appears to be weak.

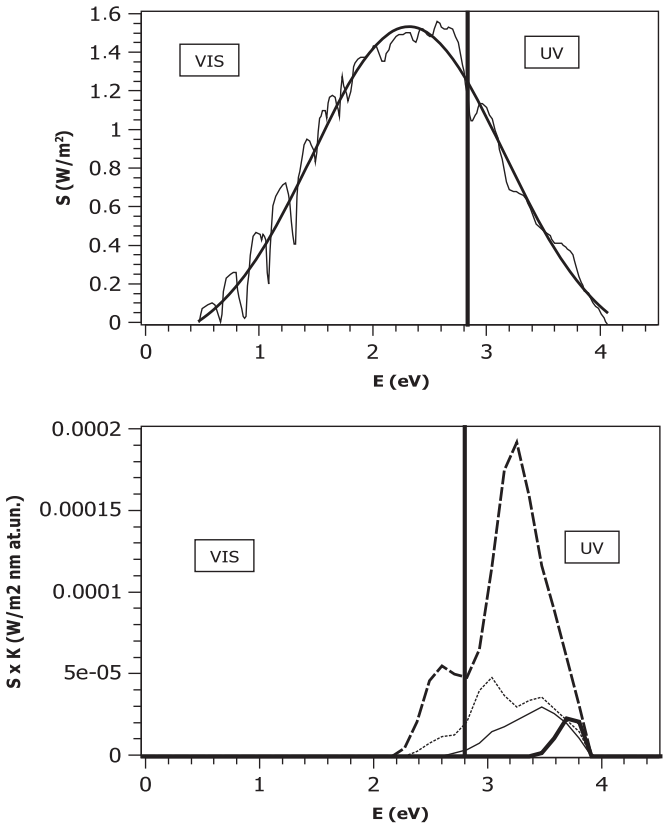

Fig. 7. Higher panel: solid line—the energy dependence of the intensity of solar radiation (S) after transmission in atmosphere, dashed line—Gaussian curve approximating the intensity of solar radiation; lower panel: absorption coefficient scaled with the intensity of solar radiation (see text). Destination of the lines is as in Figs. 5 and 6.

In Figs. 5 and 6 the values of imaginary part of dielectric function and absorption coefficient are given for V,N- and Na, N-doped anatase and for the sake of comparison for the pure anatase too. In the case of the second V,N-arrangement a noticeable change of ε_2 occurs with inclusion of crystal lattice relaxation, whereas in the rest of the cases the change of ε_2 and optical absorption with relaxation is small. In all the cases the absorption is weak in the energy interval from 2.2 to about 3 eV, but at higher energy it increases essentially with doping. For the V, N-doping this means that the impurity band-impurity band transitions only slightly contribute to the absorption, and the rise of absorption above 3 eV is provided by the transitions from the occupied impurity states to the empty states situated at the energy of $\sim$0.4 eV above the bottom of the conduction band. For the Na,N-doping the rise of absorption starts at the energy about 3.2 eV. This also corresponds to the transitions from the highest occupied impurity states to the empty states situated at about 0.5–0.6 eV above the bottom of the conduction band. Hence, the empty states in the interval of about 0−0.5 eV from the bottom of the conduction band do not take part in optical absorption. This issue was discussed in the paper [27] for the N-doped anatase. It has been shown that this effect is associated with the specific d_{xy} character of the states near the bottom of the conduction band. The lobes of the d_{xy} orbitals avoid overlap with the orbitals of the neighbor O or N atoms, thus preventing participation in optical transitions. Comparing the optical absorption in the doped anatase with that in the pure anatase we see that the edge of absorption essentially shifts with doping to lower energy. Nevertheless, in visible range the doping provides only a weak absorption, and the main effect appears to be an increase of absorption in UV region, beginning at 3 eV.

In order to evaluate the relative effectiveness of the doped anatase for the photocatalytic application, we show in Fig. 7 the absorption coefficient scaled with the Gaussian curve approximating the intensity of the sunlight spectra [48]. Evidently, this product characterizes the number of electron–hole pairs that can be excited in a compound by the sunlight radiation. The graph demonstrates the presence of absorption in visible range. Nevertheless, with all the discussed kinds of doping the main effect appears to be a great increase of the number of electron–hole pairs generated in the UV region.

Finally, it is worthwhile to notice the effect of local fields on the absorption in the doped anatase. It has been found before in the paper [49], based on the examples of $SrTiO_3$ and $BaTiO_3$, that the neglect of local fields leads to dramatically overestimation

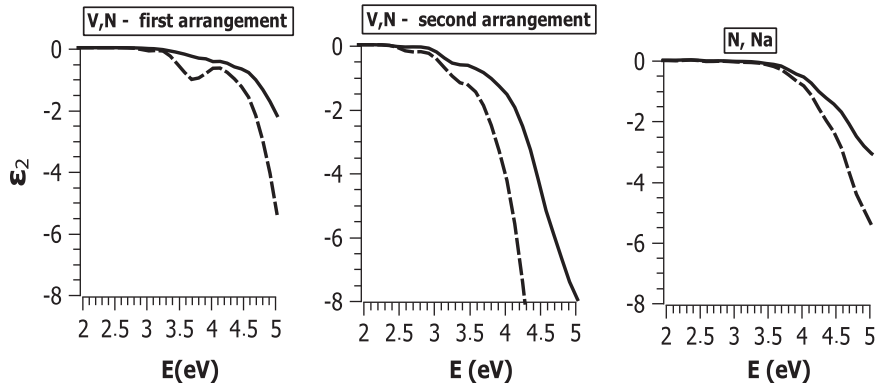

Fig. 8. The imaginary part of dielectric function for the doped anatase calculated with the local fields taken into account (solid lines) and disregarded (dashed lines). The kinds of doping elements and of atomic arrangements are shown in the panels.

of absorption. In Fig. 8 we compare the imaginary part of dielectric function for the doped anatase calculated with the local fields incorporated and also omitted. Basing on these data we come to the conclusion analogous to this of the paper [49]: the omission of the local field effects leads to an essential overestimation of the absorption in the optical range and the near UV also.

5. Conclusions

Employing the first-principle TB-LMTO approach we have studied the electronic band structure and characteristics of optical absorption in the anatase doped with nitrogen and vanadium, nitrogen and sodium. The calculations demonstrate the emergence with doping of the impurity bands inside the band gap of the anatase. Optical characteristics have been calculated with the local fields effects taken into account. The crystal lattice relaxation in the vicinity of the doping atoms has been studied by means of the pseudo-potential plane wave approach (Quantum Espresso code). We have found that the relaxation essentially affects the energy of the impurity states. We show also that the vanadium and nitrogen atoms demonstrate a trend to form covalently bonded pairs. The crystal lattice relaxation around the pairs is accompanied by an essential change of the optical absorption.

We find that the impurity band–impurity band transition introduce only small contribution to optical absorption in visible range, and the main changes of absorption occur in the UV region. The transitions from the highest occupied impurity bands to the lowest states of the conduction band are of minor importance for optical absorption.

Our calculations show that the qualitative approach of evaluating the effect of doping on the optical absorption from only the energy of the band states is for the studied compounds of very limited accuracy, and the transition probabilities should be taken into account. We demonstrate also that the neglect of the local field effects leads to overestimated absorption in the visible region and near UV, so the local fields also has to be incorporated into the calculations.

The main effect of doping on the optical absorption consists in the rise of absorption at the energy above 3 eV. Hence we conclude that the doping with nitrogen and vanadium or nitrogen and sodium should rise photocatalytic activity of anatase in the nearest UV region.

References

[1] A. Fujishima, K. Honda, Nature 238 (1972) 37.
[2] A. Fujishima, X. Zhang, C.R. Chimie 9 (2006) 750.
[3] O. Carp, C. Huisman, A. Reller, Prog. Solid State Chem. 32 (2004) 33.
[4] M. Kaneko, I. Okura, Photocatalysis: Science and Technology, Springer, New York, 2002.
[5] R. Benedix, F. Dehn, J. Quaas, M. Orgass, Laser 5 (2000) 160.
[6] E. Reddy, L. Davydov, P. Smirniotis, J. Phys. Chem. B 106 (2002) 3394.
[7] S. Amemiya, ThreeBond Technical News 62 (2004) 1.
[8] W. Zhao, W. Ma, C. Chen, J. Zhao, Z. Shuai, J. Am. Chem. Soc. 126 (2004) 4782.
[9] X. Yang, C. Cao, K. Hohn, L. Erickson, R. Maghirang, D. Hamal, K. Klabunde, J. Catal. 252 (2007) 296.
[10] V. Krasilnikov, A. Shtin, O. Girdasova, E. Poliakov, L.I. Buldakova, M. Ianchenko, V. Zainullina, V. Zhukov, Zh. Neorg. Khim. 55 (2010) 1258.
[11] R. Asahi, T. Morikawa, T. Ohwaki, K. Aoki, Y. Taga, Science 293 (2001) 269.
[12] H. Tang, H. Berger, P. Schmid, F. Levy, G. Burri, Solid State Commun. 87 (1993) 847.
[13] K. Mizushima, M. Tanaka, A. Asai, S. Iida, J.B. Goodenoug, J. Phys. Chem. Sol. 40 (1979) 1129.
[14] H. Geng, S. Yin, X. Yang, Z. Shuai, B. Liu, J. Phys. C: Condens. Matter 18 (2006) 87.
[15] K. Yang, Y. Dai, B. Huang, Phys. Rev. B 76 (2007) 195201.
[16] E. Finazzi, C.D. Valentin, G. Pacchioni, J. Phys. Chem. C 113 (2009) 220.
[17] H. Wang, J. Lewis, J. Phys. C: Condens. Matter 17 (2005) L209.
[18] T. Morikawa, R. Asahi, T. Ohwaki, K. Aoki, K. Suzuki, Y. Taga, R&D Rev. Toyota CRDL 40 (2005) 45.
[19] V. Zainullina, V. Zhukov, V. Krasilnikov, M. Ianchenko, L.I. Buldakova, E. Poliakov, Fiz. Tverd. Tela 52 (2010) 253.
[20] V. Zainullina, M. Korotin, V. Zhukov, Physica B 405 (2010) 2110.
[21] C.D. Valentin, G. Pacchioni, A. Selloni, Phys. Rev. B 70 (2004) 085116.
[22] J.-Y. Lee, J. Park, J.-H. Cho, Appl. Phys. Lett. 87 (2005) 011904.
[23] M. Long, W. Cai, Z. Wang, G. Liu, Chem. Phys. Lett. 420 (2006) 71.
[24] L. Mi, P. Xu, H. Shen, P.-N. Wanga, Appl. Phys. Lett. 90 (2007) 171909.
[25] G. Pan, Z. Xuejun, Z. Wenfang, W. Jing, L. Qingju, J. Semicond. 31 (2010) 032001.
[26] Z. Zhao, Q. Liu, J. Phys. D: Appl. Phys. 41 (2008) 025105.
[27] E.C.V.P. Zhukov, V.M. Zainullina, Int. J. Mod. Phys. 24 (2010) 6049.
[28] T. Sekiya, T. Yagisawa, N. Kamyia, D.D. Mulmi, S. Kurita, Y. Murakami, T. Kodira, J. Phys. Soc. Japan 73 (2004) 703.
[29] T. Sekiya, S. Kurita, Defects in anatase titanium dioxide, Nano- and Micromaterials, Advances in Material Research, vol. 9, Springer, Berlin, Heidelberg, 2008.
[30] F. Filippone, G. Mattioli, P. Alippi, A.A. Bonapasta, Phys. Rev. B 80 (2009) 245203.
[31] S. Bouattour, W. Kallel, A.M.B. do Rego, L.V. Ferreira, I.F. Machado, S. Boufi, Appl. Organomet. Chem. 24 (2010) 692.
[32] J. Ziman, Principles of the Theory of Solids, University Press, Cambridge, 1972.
[33] D. Pines, Elementary Excitations in Solids, Addison-Wesley, New York, 1963.
[34] A. Fetter, J. Walecka, Quantum Theory of Many-particle Systems, McGraw-Hill, New York, 1971.
[35] G. Mahan, Many-particle physics, Plenum Press, New York, 1990.
[36] F. Aryasetiawan, O. Gunnarsson, M. Knupfer, J. Fink, Phys. Rev. B 50 (1994) 7311.
[37] F. Aryasetiawan, O. Gunnarsson, Rep. Prog. Phys. 61 (1998) 237.
[38] V.P. Zhukov, E. Chulkov, P. Echenique, Phys. Rev. B 65 (2002) 115116.
[39] V.P. Zhukov, E. Chulkov, P. Echenique, Phys. Rev. Lett. 93 (2004) 096401.
[40] C. Howard, T. Sabina, F. Dickson, Acta Crystallogr. B 47 (1991) 462.
[41] O. Jepsen, G. Krier, A. Burkhardt, O.K. Andersen, The TB-LMTO-ASA program, Max-Planck-Institut für Festkörperforschung, Heisenbergstr. 1, D-70569 Stuttgart, Federal Republic of Germany, 1994.
[42] O. Andersen, O. Jepsen, M. Sob, Linearized band structure methods, in: M. Yussouff (Ed.), Electronic Band Structure and its Applications, Lecture Notes in Physics, vol. 283, Springer, 1987.
[43] V. Anisimov, J. Zaanen, O. Andersen, Phys. Rev. B 44 (1991) 943.
[44] S. Baroni, S. de Gironcoli, A.D. Corso, Rev. Mod. Phys. 73 (2001) 515.
[45] 〈http://www.quantum-espresso.org〉 and 〈http://www.pwscf.org〉, 2010.
[46] V. Zhukov, F. Aryasetiawan, E. Chulkov, I. de Gurtubay, P.M. Echenique, Phys. Rev. B 64 (2001) 195122.
[47] F. Aryasetiawan, O. Gunnarsson, Phys. Rev. B 49 (1994) 16214.
[48] R. Wayne, The Chemistry of Atmospheres, Oxford University Press, 1991.
[49] E.E. Krasovskii, W. Schattke, Phys. Rev. B 60 (1999) R16251.